

Attentive Normalization

Xilai Li, Wei Sun and Tianfu Wu *

Department of ECE and the Visual Narrative Initiative, NC State University

{xli47, wsun12, tianfu.wu}@ncsu.edu

Abstract

In state-of-the-art deep neural networks, both feature normalization and feature attention have become ubiquitous with significant performance improvement shown in a vast amount of tasks. They are usually studied as separate modules, however. In this paper, we propose a light-weight integration between, and thus harness the best of, the two schema. We present Attentive Normalization (AN) which generalizes the common affine transformation component in the vanilla feature normalization. Instead of learning a single affine transformation, AN learns a mixture of affine transformations and utilizes their weighted-sum as the final affine transformation applied to re-calibrate features in an instance-specific way. The weights are learned by leveraging feature attention. AN introduces negligible extra parameters and computational cost (i.e., light-weight). AN can be used as a drop-in replacement for any feature normalization technique which includes the affine transformation component. In experiments, we test the proposed AN using three representative neural architectures (ResNets [11], MobileNets-v2 [36] and AOGNets [24]) in the ImageNet-1000 classification benchmark [34] and the MS-COCO 2107 object detection and instance segmentation benchmark [26]. AN obtains consistent performance improvement for different neural architectures in both benchmarks with absolute increase of top-1 accuracy in ImageNet-1000 between 0.5% and 2.0%, and absolute increase up to 1.8% and 2.2% for bounding box and mask AP in MS-COCO respectively. The source codes are publicly available ¹.

1. Introduction

1.1. Motivation and Objective

Pioneered by Batch Normalization (BN) [19], feature normalization has become ubiquitous in the development

*T. Wu is the corresponding author.

¹Classification in ImageNet: <https://github.com/iVMCL/AOGNets-v2> and Detection in MS-COCO: https://github.com/iVMCL/AttentiveNorm_Detection

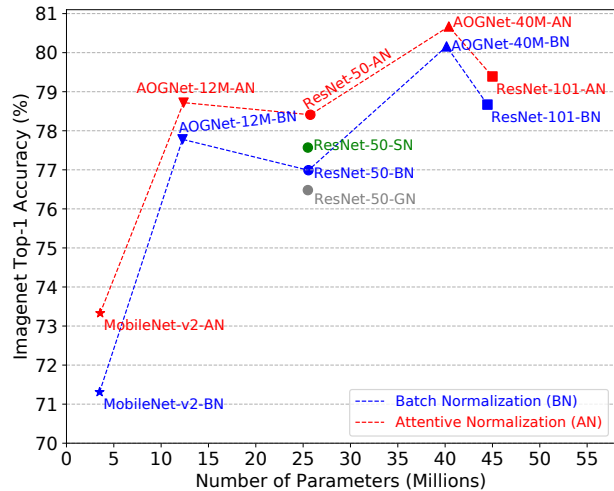


Figure 1. Performance plots for the proposed Attentive Normalization (AN) and the vanilla Batch Normalization (BN) [19] across three neural architectures, ResNets [11], MobileNets-v2 [36] and AOGNets [24] in ImageNet-1000 [34]. The proposed AN consistently improves performance. It also outperforms other variants of BN tested using ResNet-50: GroupNorm (GN) [45] and SwitchableNorm (SN) [28]. See text for details. Best viewed in color.

of deep learning. As illustrated in Figure 2, feature normalization consists of two components: *feature standardization* and *channel-wise affine transformation* which is introduced to provide the capability of undoing the standardization (by design), and can be treated as *feature re-calibration* in general. Many variants of BN have been proposed for practical deployment in terms of variations of training and testing settings with remarkable progress obtained. They can be roughly divided into two categories:

- *Generalizing feature standardization.* Different methods are proposed for computing the mean(s) and standard deviation(s), or for modeling the data distribution in general, within a min-batch. They include Batch Renormalization [18], Decorrelated BN [16], Layer Normalization (LN) [1], Instance Normalization (IN) [41], Instance-level Meta Normalization [20], Group Normalization (GN) [45], Mixture Normal-

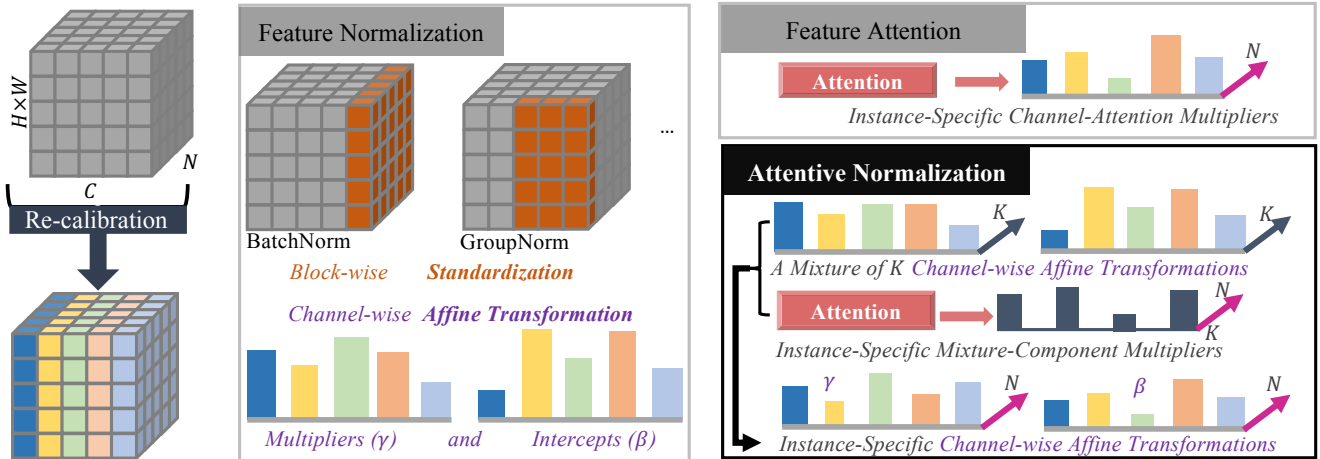


Figure 2. Illustration of the proposed Attentive Normalization (AN). AN aims to harness the best of feature normalization and feature attention. AN keeps the block-wise standardization unchanged. AN learns a mixture of K channel-wise affine transformations. AN leverages attention mechanism to learn the instance-specific weights for the mixture components in computing the weighted sum of the mixture as the final affine transformation for re-calibrating the input features. See text for details. Best viewed in color.

ization [21] and Mode Normalization [6]. Switchable Normalization (SN) [28] and its sparse variant (SSN) [38] learn to switch between different vanilla schema. These methods adopt the vanilla channel-wise affine transformation after standardization, and are often proposed for discriminative learning tasks.

- *Generalizing feature re-calibration.* Instead of treating the affine transformation parameters directly as model parameters, different types of task-induced conditions (e.g., class labels in conditional image synthesis using generative adversarial networks) are leveraged and encoded as latent vectors, which are then used to learn the affine transformation parameters, including different conditional BNs [7, 5, 32, 29, 2], style-adaptive IN [22] or layout-adaptive IN [30, 39]. These methods have been mainly proposed in generative learning tasks.

In the meanwhile, *feature attention* has also become an indispensable mechanism for improving task performance in deep learning. For computer vision, spatial attention is inherently captured by convolution operations within short-range context, and by non-local extensions [43, 17] for long-range context. Channel-wise attention is relatively less exploited. The squeeze-and-excitation (SE) unit [14] is one of the most popular designs, which learn instance-specific channel-wise attention weights to re-calibrate an input feature map (Figure 2). Unlike the affine transformation parameters in feature normalization, the attention weights for re-calibrating an feature map are often directly learned from the input feature map in the spirit of self-attention, and often instance-specific or pixel-specific.

Although both feature normalization and feature atten-

tion have become ubiquitous in state-of-the-art DNNs, they are usually studied as separate modules. Therefore, in this paper we address the following problem,

How to learn to re-calibrate feature maps in a way of harnessing the best of feature normalization and feature attention in a single light-weight module?

To that end, we present **Attentive Normalization (AN)**. our proposed AN is both conceptually and computationally simple, which can be used as a drop-in replacement for any feature normalization method that includes the affine transformation component and results in consistent performance improvement (Figure 1).

1.2. Method Overview

Figure 2 illustrates the proposed AN. The basic idea is straightforward. Conceptually, the affine transformation component in feature normalization (Section 3.1) and the re-scaling computation in feature attention play the same role in learning-to-re-calibrate an input feature map, thus providing the foundation for integration (Section 3.2). More specifically, consider a feature normalization backbone such as BN or GN, our proposed AN keeps the block-wise standardization component unchanged. Unlike the vanilla feature normalization in which the affine transformation parameters (γ 's and β 's) are often frozen in testing, we want the affine transformation parameters to be adaptive and dynamic in both training and testing, controlled directly by the input feature map. The intuition behind doing so is that it will be more flexible in accounting for different statistical discrepancies between training and testing in general, and between different sub-populations caused by underlying inter-/intra-class variations in the data.

To achieve the dynamic and adaptive control of affine transformation parameters, the proposed AN utilizes a simple design (Section 3). It learns a mixture of K affine transformations and exploits feature attention mechanism to learn the instance-specific weights for the K components. The final affine transformation used to re-calibrate an input feature map is the weighted sum of the learned K affine transformations. We propose a general formulation for the proposed AN (Section 3.3.1). We study how to learn the weights in an efficient and effective way (Section 3.3.2). We study how to deploy the proposed AN to state-of-the-art building blocks such as the Bottleneck block [11] in a light-weight manner in terms of both parameter increase and computational expense (Section 3.4).

In experiments, we focus on image classification and object detection and instance segmentation tasks. We test the proposed AN with BN and GN as the feature normalization backbones in three state-of-the-art DNNs: ResNets [11], MobileNets-v2 [36] and AOGNets [24]. We test our AN in the ImageNet-1000 dataset [34] and the MS-COCO dataset [26]. Our AN significantly outperforms the vanilla feature normalization backbones consistently across the three networks in the two datasets. We also perform an ablation study comparing different design choices in AN.

2. Related Work

Feature Normalization. There are two types of normalization schema, feature normalization (including raw data) [19, 18, 1, 41, 45, 28, 38, 21, 6] and weight normalization [35, 15]. Unlike the former stated above, the latter is to normalize model parameters to decouple the magnitudes of parameter vectors from their directions. We focus on feature normalization in this paper.

Different feature normalization schema differ in how the mean and variance are computed. BN [19] computes the channel-wise mean and variance in the entire min-batch which is driven by improving training efficiency and model generalizability. BN has been deeply analyzed in terms of how it helps optimization [37]. DecorBN [16] adds a whitening operation after the standardization. BatchReNorm [18] introduces extra parameters to control the pooled mean and variance to reduce BN’s dependency on the batch size. IN [41] focuses on channel-wise and instance-specific statistics which stems from the task of artistic image style transfer. LN [1] computes the instance-specific mean and variance from all channels which is designed to help optimization in recurrent neural networks (RNNs). GN [45] stands in the sweet spot between LN and IN focusing on instance-specific and channel-group-wise statistics, especially when only small batches are applicable in practice. In practice, synchronized BN [31] across multiple GPUs becomes increasingly favorable against GN in some applications. SN [28] leaves

the design choices of feature normalization schema to the learning system itself by computing weighted sum integration of BN, LN, IN and/or GN via softmax, showing more flexible applicability, followed by SSN [38] which learns to make exclusive selection. Instead of computing one mode (mean and variance), MixtureNorm [21] introduces a mixture of Gaussian densities to approximate the data distribution in a mini-batch. ModeNorm [6] utilizes a general form of multiple-mode computation. Unlike those methods, the proposed AN focuses on generalizing the affine transformation component. Related to our work, Instance-level Meta normalization(ILM) [20] first utilizes an encoder-decoder sub-network to learn affine transformation parameters and then add them together to the model’s affine transformation parameters. Unlike ILM, the proposed AN utilizes a mixture of affine transformations and leverages feature attention to learn the instance-specific attention weights.

On the other hand, conditional feature normalization schema [7, 5, 32, 2, 22, 30, 39] have been developed and shown remarkable progress in conditional and unconditional image synthesis. Conditional BN learns condition-specific affine transformations in terms of conditions such as class labels, image style, label maps and geometric layouts. Unlike those methods, the proposed AN learns self-attention data-driven weights for mixture components of affine transformations.

Feature Attention. Similar to feature normalization, feature attention is also an important building block in the development of deep learning. Residual Attention Network [42] uses a trunk-and-mask joint spatial and channel attention module in an encoder-decoder style for improving performance. To reduce the computational cost, channel and spatial attention are separately applied in [44]. The SE module [14] further simplifies the attention mechanism by developing a light-weight channel-wise attention method. The proposed AN leverages the idea of SE in learning attention weights, but formulates the idea in a novel way.

Our Contributions. This paper makes the following main contributions in the field of deep learning.

- It presents Attentive Normalization which harnesses the best of feature normalization and feature attention (channel-wise). To our knowledge, AN is the first work that studies self-attention based conditional and adaptive feature normalization in visual recognition tasks.
- It presents a lightweight integration method for deploying AN in the widely used Bottleneck block and its variants.
- It obtains consistently better results than the vanilla feature normalization backbones by a large margin across different neural architectures in two large-scale benchmarks, ImageNet-1000 and MS-COCO.

3. The Proposed Attentive Normalization

In this section, we present details of the proposed attentive normalization. Without loss of generality, consider a DNN for 2D images, denote by \mathbf{x} a feature map with axes in the convention order of (N, C, H, W) (i.e., batch, channel, height and width). \mathbf{x} is represented by a 4D tensor. Let $i = (i_N, i_C, i_H, i_W)$ be the address index in the 4D tensor. \mathbf{x}_i represents the feature response at a position i . Note that we can squeeze the last two dimensions to be consistent with Figure 2.

3.1. Background on Feature Normalization

As aforementioned, existing feature normalization schema often consist of two components:

i) Block-wise Standardization. Denote by B_j a block (slice) in a given 4-D tensor \mathbf{x} . For example, for BN, we have $j = 1, \dots, C$ and $B_j = \{\mathbf{x}_i | \forall i, i_C = j\}$. We first compute the empirical mean and standard deviation in B_j , denoted by μ_j and σ_j respectively, and we have,

$$\mu_j = \frac{1}{M} \sum_{x \in B_j} x, \quad \sigma_j = \sqrt{\frac{1}{M} \sum_{x \in B_j} (x - \mu_j)^2 + \epsilon}, \quad (1)$$

where $M = |B_j|$ and ϵ is a small positive constant to ensure $\sigma_j > 0$ for the sake of numeric stability. Then, let j_i be the index of the block that the position i belongs to, and we standardize the feature response by,

$$\hat{\mathbf{x}}_i = \frac{1}{\sigma_{j_i}} (\mathbf{x}_i - \mu_{j_i}) \quad (2)$$

Remark: As studied in [37], other types of data-statistics can also be exploited in standardization. Since our proposed AN keeps the standardization component unchanged, it will also be applicable to these variants.

ii) Channel-wise Affine Transformation. Denote by γ_c and β_c the scalar coefficient (re-scaling) and offset (re-shifting) parameter respectively for the c -th channel. The re-calibrated feature response at a position i is then computed by,

$$\tilde{\mathbf{x}}_i = \gamma_{i_C} \cdot \hat{\mathbf{x}}_i + \beta_{i_C}, \quad (3)$$

where γ_c 's and β_c 's are shared by all the instances in a min-batch across the spatial domain. They are usually frozen in testing and fine-tuning.

3.2. Background on Feature Attention

We focus on channel-wise attention and briefly review the Squeeze-Excitation (SE) module [14]. SE usually takes the feature normalization result (Eqn. 3) as its input. SE learns channel-wise attention weights as follows:

i) The squeeze module encodes the inter-dependencies between feature channels in a low dimensional latent space

with the reduction rate r (e.g., $r = 16$),

$$S(\tilde{\mathbf{x}}; \theta_S) = v, \quad v \in \mathbb{R}^{N \times \frac{C}{r} \times 1 \times 1}, \quad (4)$$

which is implemented by a sub-network consisting of a global average pooling layer (AvgPool), a fully-connected (FC) layer and rectified linear unit (ReLU) [23]. θ_S collects all the model parameters.

ii) The excitation module computes the channel-wise attention weights, denoted by λ , by decoding the learned latent representations v ,

$$E(v; \theta_E) = \lambda, \quad \lambda \in \mathbb{R}^{N \times C \times 1 \times 1}, \quad (5)$$

which is implemented by a sub-network consisting of a FC layer and a sigmoid layer. θ_E collects all model parameters.

Then, the input, $\tilde{\mathbf{x}}$ is re-calibrated by,

$$\begin{aligned} \tilde{\mathbf{x}}_i^{SE} &= \lambda_{i_N, i_C} \cdot \tilde{\mathbf{x}}_i, \\ &= (\lambda_{i_N, i_C} \cdot \gamma_{i_C}) \cdot \hat{\mathbf{x}}_i + \lambda_{i_N, i_C} \cdot \beta_{i_C}, \end{aligned} \quad (6)$$

where the second step is obtained by plugging in Eqn. 3. It is straightforward to see the foundation facilitating the integration between feature normalization and channel-wise feature attention. However, the SE module often entails a significant number of extra parameters (e.g., $\sim 2.5M$ extra parameters for ResNet-50 [11] which originally consists of $\sim 25M$ parameters, resulting in 10% increase). We aim to design more parsimonious integration that can further improve performance (i.e., favoring ‘‘less is more’’).

3.3. Attentive Normalization

3.3.1 The Formulation

Our goal is to generalize Eqn. 3 in re-calibrating feature responses to enable dynamic and adaptive control in both training and testing. On the other hand, our goal is to simplify Eqn. 6 into a single light-weight module, rather than, for example, the two-module setup using BN+SE. In the most general form, we have,

$$\tilde{\mathbf{x}}_i^{AN} = \Gamma(\mathbf{x}; \theta_\Gamma)_i \cdot \hat{\mathbf{x}}_i + \mathbb{B}(\mathbf{x}; \theta_\mathbb{B})_i, \quad (7)$$

where both $\Gamma(\mathbf{x}; \theta_\Gamma)$ and $\mathbb{B}(\mathbf{x}; \theta_\mathbb{B})$ are functions of the entire input feature map (without standardization²) with parameters θ_Γ and $\theta_\mathbb{B}$ respectively. The two functions compute 4-D tensors of the size same as the input feature map and can be parameterized by some attention guided light-weight DNNs. The subscript in $\Gamma(\mathbf{x}; \theta_\Gamma)_i$ and $\mathbb{B}(\mathbf{x}; \theta_\mathbb{B})_i$ represents the learned re-calibration weights at a position i .

In this paper, we focus on learning instance-specific channel-wise affine transformations. To that end, we have three components as follows.

²We tried the variant of learning $\Gamma()$ and $\mathbb{B}()$ from the standardized features and observed it works worse, so we ignore it in our experiments.

i) *Learning a Mixture of K Channel-wise Affine Transformations.* Denote by $\gamma_{k,c}$ and $\beta_{k,c}$ the re-scaling and re-shifting (scalar) parameters respectively for the c -th channel in the k -th mixture component. They are model parameters learned end-to-end via back-propagation.

ii) *Learning Attention Weights for the K Mixture Components.* Denote by $\lambda_{n,k}$ the instance-specific mixture component weight ($n \in [1, N]$ and $k \in [1, K]$), and by λ the $N \times K$ weight matrix. λ is learned via some attention-guided function from the entire input feature map,

$$\lambda = A(\mathbf{x}; \theta_\lambda), \quad (8)$$

where θ_λ collects all the parameters.

iii) *Computing the Final Affine Transformation.* With the learned $\gamma_{k,c}$, $\beta_{k,c}$ and λ , the re-calibrated feature response is computed by,

$$\tilde{\mathbf{x}}_i^{AN} = \sum_{k=1}^K \lambda_{i_N,k} [\gamma_{k,i_C} \cdot \tilde{\mathbf{x}}_i + \beta_{k,i_C}], \quad (9)$$

where $\lambda_{i_N,k}$ is shared by the re-scaling parameter and the re-shifting parameter for simplicity. Since the attention weights λ are adaptive and dynamic in both training and testing, the proposed AN realizes adaptive and dynamic feature re-calibration. Compared to the general form (Eqn. 7), we have,

$$\Gamma(\mathbf{x})_i = \sum_{k=1}^K \lambda_{i_N,k} \cdot \gamma_{k,i_C}, \quad \mathbb{B}(\mathbf{x})_i = \sum_{k=1}^K \lambda_{i_N,k} \cdot \beta_{k,i_C}, \quad (10)$$

from which we can see two main advantages of the proposed AN in both training, fine-tuning and testing:

- γ_{k,i_C} 's and β_{k,i_C} 's are channel-wise and shared across spatial dimensions and by data instances, which can learn population-level knowledge. $\lambda_{i_N,k}$'s are instance specific and learned from features that are not standardized. Combining them together enables paying attention to both the population (what the common and useful information are) and the individuals (what the specific yet critical information are). The latter is particularly useful for testing samples "drifted" from training population, that is to improve generalizability. It also helps establish more direct connections between standardization and affine transformation in feature normalization. Their weighted sum encodes more direct and "actionable" information for re-calibrating standardized features (Eqn. 9) without being delayed until back-propagation updates as done in the vanilla feature normalization.
- In fine-tuning, especially between different tasks (e.g., from image classification to object detection), γ_{k,i_C} 's and β_{k,i_C} 's are usually frozen as done in the vanilla

feature normalization. They carry information from the source tasks. But, θ_λ (Eqn. 8) are allowed to be fine-tuned, thus potentially better realizing transfer learning for the target tasks. This is a desirable property since we can decouple training correlation between tasks. For example, it is not necessary to train a model in ImageNet with the feature normalization scheme such as GN [45] that is practically feasible and beneficial in object detection in MS-COCO. As we shall show in experiments, the proposed AN facilitates a smoother transition. We can use the proposed AN with BN as normalization backbone in pre-training in ImageNet, and then use AN with GN as normalization backbone for the head classifiers in MS-COCO with significant improvement.

3.3.2 Details of Learning Attention Weights

We present a simple method for computing the attention weights $A(\mathbf{x}; \theta_\lambda)$ (Eqn. 8). Our goal is to learn a weight coefficient for each component from each individual instance in a mini-batch (i.e, a $N \times K$ matrix). The question of interest is how to characterize the underlying importance of a channel c from its realization across the spatial dimensions (H, W) in an instance, such that we will learn a more informative instance-specific weight coefficient for a channel c in re-calibrating the feature map \mathbf{x} .

In realizing Eqn. 8, the proposed method is similar in spirit to the squeeze module in SE to maintain light-weight implementation. To show the difference, let's first rewrite the vanilla squeeze module (Eqn. 4),

$$v = S(\mathbf{x}; \theta_S) = \text{ReLU}(fc(\text{AvgPool}(\mathbf{x}); \theta_S)), \quad (11)$$

where the mean of a channel c (via global average pooling, $\text{AvgPool}(\cdot)$) is used to characterize its underlying importance. We generalize this assumption by taking into account both mean and standard deviation empirically computed for a channel c , denoted by μ_c and σ_c respectively (μ_c and σ_c are computed using Eqn. 1 under the BN setting). More specifically, we compare three different designs using:

- The mean μ_c only as done in SE.
- The concatenation of the mean and standard deviation, (μ_c, σ_c) .
- The coefficient of variation or the relative standard deviation (RSD), $\frac{\mu_c}{\sigma_c}$.

RSD measures the dispersion of an underlying distribution (i.e., the extent to which the distribution is stretched or squeezed) which intuitively conveys more information in learning attention weights for re-calibration. RSD is indeed

observed to work better in our experiments. Eqn. 8 is then expanded with two choices,

$$\text{Choice 1: } A_1(\mathbf{x}; \theta_\lambda) = \text{Act}(fc(RSD(\mathbf{x}); \theta_\lambda)), \quad (12)$$

$$\text{Choice 2: } A_2(\mathbf{x}; \theta_\lambda) = \text{Act}(BN(fc(RSD(\mathbf{x}); \theta_{fc}); \theta_{BN})),$$

where $\text{Act}(\cdot)$ represents a non-linear activate function for which we compare three designs:

- i) The vanilla $\text{sigmoid}(\cdot)$ as used in the excitation module of SE.
- ii) The channel-wise $\text{softmax}(\cdot)$.
- iii) the piece-wise linear hard analog of the sigmoid function, so-called h-sigmoid function [13],

$$hsigmoid(a) = ReLu6(a + 3.0)/6.0,$$

where $ReLu6(a) = \min(\max(a, 0), 6.0)$ is a variant of the vanilla ReLu function with a saturation threshold 6.0.

The $hsigmoid(\cdot)$ is observed to work better in our experiments. In the Choice 2 (Eqn. 12), we apply the vanilla BN [19] after the FC layer, which normalizes the learned attention weights across all the instances in a mini-batch with the hope of balancing the instance-specific attention weights better. The Choice 2 improves performance in our experiments in ImageNet.

During the learning, we have another hyper-parameter, K . For stage-wise building block based neural architectures such as ResNets [11], we use different K 's for different stages with smaller values for early stages. For example, for the 4-stage ResNets, we typically use $K = 10, 10, 20, 20$ for the four stages respectively to balance the expressive power of the mixture of affine transformations and the expense (we are interested in making extra parameters and computation cost negligible).

Learning the attention weights $A(\mathbf{x}; \theta_\lambda)$ can adopt other implementations when deploying in different domains such as in NLP. It can also leverage more effective and efficient channel-wise attention mechanism when available in future.

3.4. Integrating AN in Building Blocks of DNNs

In general, the proposed AN can be used as a drop-in replacement for all feature normalization layers in a DNN. Typically, in convolutional neural networks (ConvNets), a feature normalization layer follows a convolution layer. It is not necessary to replace all vanilla feature normalization layers for two reasons: First, our AN exploits feature attention to re-calibrate an input feature map, which is not needed for every convolution layer in a ConvNet, especially for 1×1 convolution which only handles feature channels (increasing or decreasing), and thus channel-wise recalibration can be tackled by the convolution kernel and the

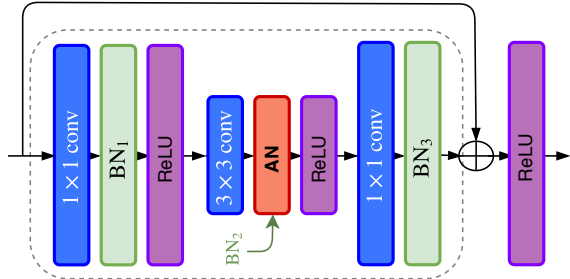


Figure 3. Illustration of integrating the proposed AN in the popular Bottleneck building block presented in ResNets [11]. Here, the feature normalization backbone is BN. The proposed AN is only used to replace the second one (BN₂) followed the 3×3 convolution. This leads to negligible extra parameters. Furthermore, this potentially enables jointly integrating local spatial attention in learning the instance-specific attention weights.

vanilla feature normalization themselves in training. Second, adding too many AN layers may make a ConvNet computationally sloppy. Consider the widespread of the Bottleneck block [11] in ConvNets, we integrate one AN layer into one Bottleneck block, as illustrated and explained in Figure 3. The integration of SE adopts the same practice and uses the spot after BN₃ in a Bottleneck block.

4. Experiments

In this section, we first show the ablation study verifying the aforementioned design choices we used in the proposed AN. Then, we present detailed comparisons and results. *Our reproducible code will be released soon.*

Data and Evaluation Metric. In experiments, we use two benchmarks, the ImageNet-1000 classification benchmark (ILSVRC2012) [34] and the MS-COCO object detection and instance segmentation benchmark [26]. The ImageNet-1000 benchmark consists of about 1.28 million images for training, and 50,000 for validation, from 1,000 classes. We apply a single-crop with size 224×224 in evaluation. Following the common protocol, we report the top-1 and top-5 classification error rates tested using a single model on the validation set. For the MS-COCO benchmark, there are 80 categories of objects. We use `train2017` in training and evaluate the trained models using `val2017`. We report the standard COCO metrics of Average Precision (AP) at different intersection-over-union (IoU) thresholds, e.g., AP₅₀ and AP₇₅, for bounding box detection (AP^{bb}_{IoU}) and instance segmentation (AP^m_{IoU}), and the mean AP over IoU=0.5 : 0.05 : 0.75, AP^{bb} and AP^m for bounding box detection and instance segmentation respectively.

Neural Architectures and Feature Normalization Backbones. We use three representative neural architectures: (i) ResNets [11] (ResNet-50 and ResNet-101), which are the most widely used architectures in practice,

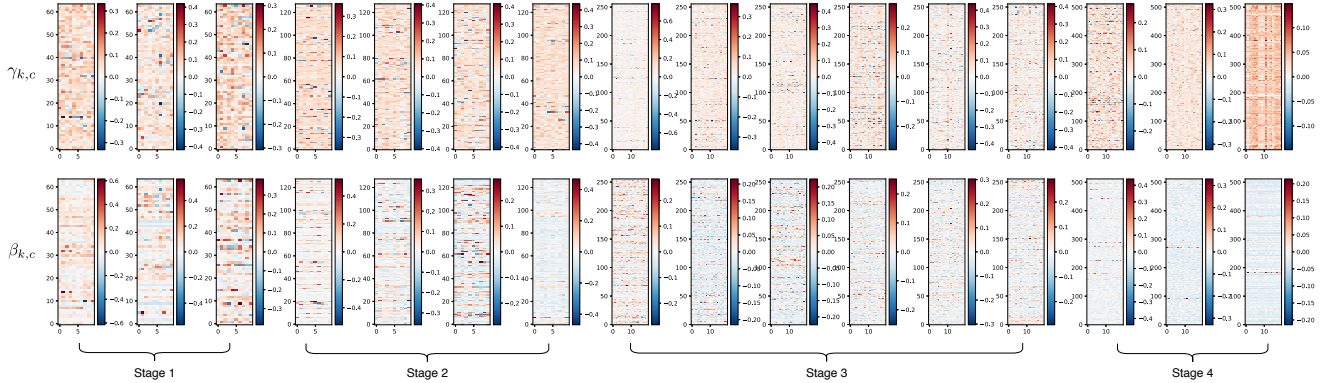


Figure 4. Heatmap visualization of γ_{k,i_C} 's and β_{k,i_C} 's in the AN. See text for details. Best viewed in color and magnification.

(ii) MobileNet-v2 [36]. MobileNets are popular architectures under mobile settings and MobileNet-v2 uses inverted residuals and linear Bottlenecks (for which our AN follows the 3×3 convolution layer in the way same as Figure 3), and (iii) AOGNets [24] (AOGNet-12M and AOGNet-40M) are grammar-guided networks with the vanilla Bottleneck building block, which represent an interesting direction of network architecture engineering with better performance than ResNets and its variants shown. So, the improvement by our AN will be both broadly useful for existing ResNets/MobileNets based deployment in practice and potentially insightful for on-going and future development of more advanced and more powerful DNNs in the community. In classification, we use BN [19] as the feature normalization backbone for our proposed AN, denoted by AN (w/ BN). We compare with the vanilla BN, GN [45] and SN [28]. In object detection and instance segmentation, we use the Mask-RCNN framework [9] and its cascade variant [3] in the MMDetection code platform [4]. We fine-tune feature backbones pretrained on the ImageNet-1000 dataset. We also test the proposed AN using GN as the feature normalization backbone, denoted by AN (w/ GN) in the head classifier of Mask-RCNN.

Initialization of our AN. The initialization of $\gamma_{k,c}$'s and $\beta_{k,c}$'s (Eqn. 9) is based on, $\gamma_{k,c} = 1.0 + \mathcal{N}(0, 1) \times 0.1$ and $\beta_{k,c} = \mathcal{N}(0, 1) \times 0.1$, where $\mathcal{N}(0, 1)$ represents the standard Gaussian distribution. This type of initialization is also adopted for conditional BN used in the BigGAN [2].

4.1. Ablation Study

We compare different design choices in our proposed AN using ResNet-50 in ImageNet-1000. Table 1 summarizes the results. The ablation study is in support of the intuitions we have in elaborating the proposed AN in Section 3.3.2. All the models are trained using the same settings (the vanilla setup in Section 4.2).

Figure 4 shows the learned mixture of affine transformations ($\gamma_{k,c}$'s and $\beta_{k,c}$'s in each building block) in the

| Design Choices in AN (w/ BN) | #Params | FLOPS | top-1 | top-5 |
|---|---------|-------|--------------|-------------|
| RSD(mean/std) + $A_2(\cdot)$ + hsigmoid + $K = \begin{pmatrix} 10 \\ 10 \\ 20 \\ 20 \end{pmatrix}$ | 25.76M | 4.09G | 21.59 | 5.58 |
| mean + $A_2(\cdot)$ + hsigmoid + $K = \begin{pmatrix} 10 \\ 10 \\ 20 \\ 20 \end{pmatrix}$ | 25.76M | 4.09G | 21.85 | 5.92 |
| concat(mean,std) + $A_2(\cdot)$ + hsigmoid + $K = \begin{pmatrix} 10 \\ 10 \\ 20 \\ 20 \end{pmatrix}$ | 25.82M | 4.09G | 21.73 | 5.85 |
| RSD(mean/std) + $A_1(\cdot)$ + hsigmoid + $K = \begin{pmatrix} 10 \\ 10 \\ 20 \\ 20 \end{pmatrix}$ | 25.76M | 4.09G | 21.76 | 6.05 |
| RSD(mean/std) + $A_2(\cdot)$ + softmax + $K = \begin{pmatrix} 10 \\ 10 \\ 20 \\ 20 \end{pmatrix}$ | 25.76M | 4.09G | 21.72 | 5.90 |
| RSD(mean/std) + $A_2(\cdot)$ + sigmoid + $K = \begin{pmatrix} 10 \\ 10 \\ 20 \\ 20 \end{pmatrix}$ | 25.76M | 4.09G | 21.96 | 5.91 |
| RSD(mean/std) + $A_2(\cdot)$ + hsigmoid + $K = \begin{pmatrix} 5 \\ 5 \\ 10 \\ 10 \end{pmatrix}$ | 25.76M | 4.09G | 21.92 | 5.93 |
| RSD(mean/std) + $A_2(\cdot)$ + hsigmoid + $K = \begin{pmatrix} 10 \\ 20 \\ 40 \\ 40 \end{pmatrix}$ | 25.96M | 4.09G | 21.62 | 5.63 |

Table 1. Ablation study on different design choices in our proposed AN with BN as feature normalization backbone using ResNet-50 in ImageNet-1000. There are four categories: The first three are detailed in Section 3.3.2. The fourth one refers to the number K of components in the mixture of affine transformation which is used for each of the four stages in ResNet-50 and we empirically select three options for simplicity. The second row shows the best design combination we observed, which will be used in our comparison experiments. In each test (row 3 to 9), we only change one in the best design combination for computational feasibility. During our development, we first observed the best combination based on our intuitive reasoning and small experiments (a few epochs) in the process, and then design this ablation study to verify the design choices. The performance of the baseline ResNet-50+BN is in Table 2. See text for details.

ResNet-50+AN (the best performer in Table 1). We can see there are no degenerated cases observed in the learned affine transformations (i.e., no single mixture component that dominates).

4.2. Image Classification in ImageNet-1000

Common Training Settings. We use 8 GPUs (NVIDIA V100) to train models using the same settings for apple-to-apple comparisons. The method proposed in [10] is used to initialize all convolutions for all models. The batch size

| Method | #Params | FLOPS | top-1 | top-5 |
|--------------------------------|---------|-------|--------------------------------|-------------------------------|
| ResNet-50-BN | 25.56M | 4.09G | 23.01 _(1.42) | 6.68 _(0.80) |
| † ResNet-50-GN [45] | 25.56M | 4.09G | 23.52 _(1.93) | 6.85 _(0.97) |
| † ResNet-50-SN [28] | 25.56M | - | 22.43 _(0.83) | 6.35 _(0.47) |
| † ResNet-50-SE [14] | 28.09M | - | 22.37 _(0.78) | 6.36 _(0.48) |
| ResNet-50-AN (w/ BN) | 25.76M | 4.09G | 21.59 | 5.88 |
| ResNet-101-BN | 44.57M | 8.12G | 21.33 | 5.85 |
| ResNet-101-AN (w/ BN) | 45.00M | 8.12G | 20.61 _(0.72) | 5.41 _(0.44) |
| MobileNet-v2-BN | 3.50M | 0.34G | 28.69 | 9.33 |
| MobileNet-v2-AN (w/ BN) | 3.56M | 0.34G | 26.67 _(2.02) | 8.56 _(0.77) |
| AOGNet-12M-BN | 12.26M | 2.19G | 22.22 | 6.06 |
| AOGNet-12M-AN (w/ BN) | 12.37M | 2.19G | 21.28 _(0.94) | 5.76 _(0.30) |
| AOGNet-40M-BN | 40.15M | 7.51G | 19.84 | 4.94 |
| AOGNet-40M-AN (w/ BN) | 40.39M | 7.51G | 19.33 _(0.51) | 4.72 _(0.22) |

Table 2. Comparisons of the top-1 and top-5 error rates (%) in the ImageNet-1000 validation set using *the vanilla setup*. The numbers in brackets show the performance improvement by our proposed AN over the baselines (for ResNet-50, the numbers are shown with the baseline methods since there are multiple ones). † means the model is not trained by us. All other models are trained from scratch by us under the same settings. See text for details.

is 128 per GPU³ with FP16 optimization used in training to reduce the training time⁴. The mean and standard deviation for block-wise standardization are computed *within* each GPU. The initial learning rate is 0.4, and the cosine learning rate scheduler [27] is used with 5 warm-up epochs and weight decay 1×10^{-4} and momentum 0.9. For AN, the best practice observed in our ablation study (Table 1) is used. AN is also used in the stem layer in the models. In addition to the common settings, we have two different setups in experimental comparisons:

i) The Vanilla Setup. We adopt the basic data augmentation scheme (random crop and horizontal flip) in training as done in [11]. We train the models for 120 epochs. All ResNets [11] use the vanilla stem layer with 7×7 convolution. The MobileNets-v2 uses 3×3 convolution in the stem layer. The AOGNets use two consecutive 3×3 convolution in the stem layer. All the γ and β parameters of the feature normalization backbones are initialized to 1 and 0 respectively.

ii) The State-of-the-Art Setup. There are different aspects in the vanilla setup which have better variants developed with better performance shown [12]. *We want to address whether the improvement by our proposed AN are truly fundamental or will disappear with more advanced tips and tricks added in training ConvNets.* First, on top of the basic data augmentation, we also use label smoothing [40] (with rate 0.1) and the mixup (with rate 0.2) [46]. We increase the total number of epochs to 200. We use the same stem layer with two consecutive 3×3 convolution for all models. We add the zero γ initialization trick for the feature normal-

³Although the best practice is to use 8 GPUs and batch size 32 per GPU for training ConvNets in ImageNet, we do not follow it since it would take too long in order to run all the experiments given the resources we have.

⁴The NVIDIA APEX library is used.

| Method | #Params | FLOPS | top-1 | top-5 |
|------------------------------|---------|-------|--------------------------------|-------------------------------|
| ResNet-50-BN | 25.56M | 4.09G | 21.08 | 5.56 |
| ResNet-50-AN (w/ BN) | 25.76M | 4.09G | 19.92 _(1.16) | 5.04 _(0.52) |
| ResNet-101-BN | 44.57M | 8.12G | 19.71 | 4.89 |
| ResNet-101-AN (w/ BN) | 45.00M | 8.12G | 18.85 _(0.86) | 4.63 _(0.26) |
| AOGNet-12M-BN | 12.26M | 2.19G | 21.63 | 5.60 |
| AOGNet-12M-AN (w/ BN) | 12.37M | 2.19G | 20.57 _(1.06) | 5.38 _(0.22) |
| AOGNet-40M-BN | 40.15M | 7.51G | 18.70 | 4.47 |
| AOGNet-40M-AN (w/ BN) | 40.39M | 7.51G | 18.13 _(0.57) | 4.26 _(0.21) |

Table 3. Comparisons of the top-1 and top-5 error rates (%) in the ImageNet-1000 validation set using *the state-of-the-art setup*. The numbers in brackets show the performance improvement by our proposed AN over the baselines. All models are trained from scratch under the same settings. See text for details.

ization backbones (not for AN), which uses 0 to initialize the last normalization layer (BN₃ in Figure 3) to make the initial state of a residual block to be identity.

Results Summary. Table 2 and Table 3 show the comparison results for the two setups respectively. **Our proposed AN consistently obtains the best top-1 and top-5 accuracy results with more than 0.5% absolute top-1 accuracy increase (up to 2.0%) in all models without bells and whistles.** *The improvement is obtained with negligible extra parameters* (e.g., 0.06M parameter increase in MobileNet-v2 for 2.02% absolute top-1 accuracy increase, and 0.2M parameter increase in ResNet-50 with 1.42% absolute top-1 accuracy increase) *at almost no extra computational cost* (up to the precision used in measuring FLOPs). With ResNet-50, our AN also outperforms GN [45] and SN [28] by 1.93% and 0.83% in top-1 accuracy respectively. For GN, it is known that it works (slightly) worse than BN under the normal (big) mini-batch setting [45]. For SN, our result shows that it is more beneficial to improve the recalibration component than to learn-to-switch between different feature normalization schema. It may be useful to integrate our AN and the SN in future work.

Remarks. We observe that the proposed AN is more effective for small ConvNets in terms of performance gain. Intuitively, this makes sense. Small ConvNets usually learn less expressive features. With the mixture of affine transformations and the instance-specific channel-wise feature recalibration, the proposed AN offers the flexibility of clustering intra-class data better while separating inter-class data better in training. This is potentially very useful in state-of-the-art neural architecture search under mobile settings. The proposed AN can be included as a strong inductive bias in the search space for learning potentially more powerful networks. In the meanwhile, the proposed AN entails a second thought on the Fixup initialization [47] which attempts to remove BN without hurting the performance. Our results show it is beneficial to improve the vanilla feature normalization schema in a light-weight manner. It will be interesting to investigate the potential integration between our

| Architecture | Backbone | Head | #Params | AP ^{bb} | AP ₅₀ ^{bb} | AP ₇₅ ^{bb} | AP ^m | AP ₅₀ ^m | AP ₇₅ ^m |
|--------------|------------|------------|---------|------------------------------|--------------------------------|--------------------------------|------------------------------|-------------------------------|-------------------------------|
| MobileNet-v2 | ℳBN | - | 22.72M | 34.2 | 54.6 | 37.1 | 30.9 | 51.1 | 32.6 |
| | AN (w/ BN) | - | 22.78M | 36.0 _(1.8) | 57.0 _(2.4) | 38.9 _(1.8) | 32.5 _(1.6) | 53.8 _(2.7) | 34.5 _(1.9) |
| ResNet-50 | ℳBN | - | 45.71M | 39.2 | 60.0 | 43.1 | 35.2 | 56.7 | 37.6 |
| | AN (w/ BN) | - | 45.91M | 40.8 _(1.6) | 62.1 _(2.1) | 44.5 _(1.4) | 36.4 _(1.2) | 58.9 _(2.2) | 38.7 _(1.1) |
| | †GN | GN [45] | 45.72M | 40.3 _(1.3) | 61.0 _(1.0) | 44.0 _(1.7) | 35.7 _(1.7) | 57.9 _(1.6) | 37.7 _(2.2) |
| | †SN | SN [28] | - | 41.0 _(0.6) | 62.3 _(-0.3) | 45.1 _(0.6) | 36.5 _(0.9) | 58.9 _(0.6) | 38.7 _(1.2) |
| | AN (w/ BN) | AN (w/ GN) | 45.96M | 41.6 | 62.0 | 45.7 | 37.4 | 59.5 | 39.9 |
| ResNet-101 | ℳBN | - | 64.70M | 41.4 | 62.0 | 45.5 | 36.8 | 59.0 | 39.1 |
| | AN (w/ BN) | - | 65.15M | 43.1 _(1.7) | 64.1 _(2.1) | 47.3 _(1.8) | 38.2 _(1.4) | 61.0 _(2.0) | 40.7 _(1.6) |
| | †GN | GN [45] | 64.71M | 41.8 | 62.5 | 45.4 | 36.8 | 59.2 | 39.0 |
| | AN (w/ BN) | AN (w/ GN) | 65.20M | 43.2 _(1.4) | 64.0 _(1.5) | 47.3 _(1.9) | 38.8 _(2.2) | 61.3 _(2.1) | 41.6 _(2.6) |
| AOGNet-12M | ℳBN | - | 33.09M | 40.7 | 61.4 | 44.6 | 36.4 | 58.4 | 38.8 |
| | AN (w/ BN) | - | 33.21M | 42.0 _(1.3) | 63.1 _(1.7) | 46.1 _(1.5) | 37.8 _(1.4) | 60.1 _(1.7) | 40.4 _(1.6) |
| | AN (w/ BN) | AN (w/ GN) | 33.26M | 43.0 _(1.0) | 64.2 _(1.1) | 46.8 _(0.7) | 38.7 _(0.9) | 61.1 _(1.0) | 41.7 _(1.3) |
| AOGNet-40M | ℳBN | - | 60.73M | 43.4 | 64.2 | 47.5 | 38.5 | 61.0 | 41.4 |
| | AN (w/ BN) | - | 60.97M | 44.1 _(0.7) | 65.1 _(0.9) | 48.2 _(0.7) | 39.0 _(0.5) | 62.0 _(1.0) | 41.8 _(0.4) |
| | AN (w/ BN) | AN (w/ GN) | 61.02M | 44.9 _(0.8) | 66.2 _(1.1) | 49.1 _(0.9) | 40.2 _(1.2) | 63.2 _(1.2) | 43.3 _(1.5) |

Table 4. Detection and segmentation results in MS-COCO val₂₀₁₇ [26] using the Mask R-CNN [9] framework with the FPN [25] implemented in MMDetection [4]. All models use 2x lr scheduling (180k iterations). ℳBN means BN is frozen in fine-tuning for object detection. † means that models are not trained by us. All other models are trained from scratch by us under the same settings (fine-tuned from pre-trained models under the vanilla setup in Table 2 for fair comparisons). The numbers in brackets show the performance improvement by our proposed AN over the baselines (the numbers show sequential improvement in the two AOGNet models).

| Architecture | Backbone | Head | #Params | AP ^{bb} | AP ₅₀ ^{bb} | AP ₇₅ ^{bb} | AP ^m | AP ₅₀ ^m | AP ₇₅ ^m |
|--------------|------------|------|---------|------------------------------|--------------------------------|--------------------------------|------------------------------|-------------------------------|-------------------------------|
| ResNet-101 | ℳBN | - | 96.32M | 44.4 | 62.5 | 48.4 | 38.2 | 59.7 | 41.3 |
| | AN (w/ BN) | - | 96.77M | 45.8 _(1.4) | 64.3 _(1.8) | 49.8 _(1.4) | 39.6 _(1.4) | 61.7 _(2.0) | 42.7 _(1.4) |
| AOGNet-40M | ℳBN | - | 92.35M | 45.6 | 63.9 | 49.7 | 39.3 | 61.2 | 42.7 |
| | AN (w/ BN) | - | 92.58M | 46.5 _(0.9) | 65.0 _(1.1) | 50.8 _(1.1) | 40.0 _(0.7) | 62.3 _(1.1) | 43.1 _(0.4) |

Table 5. Results in MS-COCO using the state-of-the-art cascade variant [3] of Mask R-CNN.

AN and the Fixup. Our AN also provides an alternative for further studying how the normalization schema helps optimization as done in [37]. We leave these for the further work.

4.3. Object Detection and Segmentation in COCO

In object detection and segmentation, high-resolution input images are beneficial and often entailed for detecting medium to small objects, but limit the batch-size in training (often 1 or 2 images per GPU). GN [45] and SN [28] have shown significant progress in handling the applicability discrepancies of feature normalization schema from ImageNet to MS-COCO. We test our AN in MS-COCO following the standard protocol as done in GN [45] and as implemented in the MMDetection code platform [4] with significant improvement obtained. The results are summarized in Table 4 and Table 5.

We first summarize the details of implementation. Following the terminologies used in MMDetection [4], there are four modular components in the R-CNN detection framework [8, 33, 9]:

- *Feature Backbone.* We use the pre-trained networks in

Table 2 (with the vanilla setup) for fair comparisons in detection, since we compare with some models which are not trained by us from scratch and use the feature backbones pre-trained in a way similar to our vanilla setup and with on par top-1 accuracy. In fine-tuning a network with AN (w/ BN) pre-trained in ImageNet such as ResNet-50+AN (w/ BN) in Table 2, we freeze the stem layer and the first stage as commonly done in practice (e.g. all the models in our experiments). For the remaining stages, we freeze the standardization component only (the learned mixture of affine transformations and the learned running mean and standard deviation), and allow the attention weight sub-network to be fine-tuned.

- *Neck Backbone.* We test the feature pyramid network (FPN) [25] which is widely used in practice.
- *Head Classifiers.* We test two setups: (i) *The vanilla setup* as done in GN [45] and SN [28]. In this setup, we further have two settings: with vs without feature normalization in the bounding box head classifier. The former is denoted by “-” in Table 4, and the latter is denoted by the corresponding type of feature normaliza-

tion scheme in Table 4 (e.g., GN, SN and AN (w/ GN)). We experiment on using AN (w/ GN) in the bounding box head classifier and keeping GN in the mask head unchanged for simplicity. Adding AN (w/ GN) in the mask head classifier may further help improve the performance. When adding AN (w/ GN) in the bounding box head, we adopt the same design choices except for “Choice 1, $A_1(\cdot)$ ” (Eqn. 12) used in learning attention weights. (ii) *The state-of-the-art setup* which is based on the cascade generalization of head classifiers [3] and does not include feature normalization scheme, also denoted by “-” in Table 5.

- *RoI Operation.* We test the RoIAlign operation [9], the default setup in Mask R-CNN.

Compared with the vanilla BN that are frozen in fine-tuning, our AN (w/ BN) improves performance by a large margin in terms of both bounding box AP and mask AP (1.8% & 1.6% for MobileNet-v2, 1.6% & 1.2% for ResNet-50, 1.7% & 1.4% for ResNet-101, 1.3% & 1.4% for AOGNet-12M and 0.7% & 0.5% for AOGNet-40M). It shows the advantages of the self-attention based dynamic and adaptive control of the mixture of affine transformations (although they themselves are frozen) in fine-tuning.

When the AN is further integrated in the bounding box head classifier of Mask-RCNN and trained from scratch, we also obtain better performance than GN and SN. Compared with the vanilla GN [45], our AN (w/ GN) improves bounding box and mask AP by 1.3% and 1.7% for ResNet-50, and 1.4% and 2.2% for ResNet-101. Compared with SN [28] which outperforms the vanilla GN in ResNet-50, our AN (w/ GN) is also better by 0.6% bounding box AP and 0.9% mask AP increase respectively. Slightly less improvements are observed with AOGNets.

Similar in spirit to the ImageNet experiments, we want to verify whether the advantages of our AN will disappear if we use state-of-the-art designs for head classifiers of R-CNN such as the widely used cascade R-CNN [3]. Table 5 shows that similar improvements are obtained with ResNet-101 and AOGNet-40M.

5. Conclusion

This paper presents Attentive Normalization (AN) that harnesses the best of feature normalization and feature attention in a single lightweight module. AN learns a mixture of affine transformations and uses the weighted sum via a self-attention module for re-calibrating standardized features in a dynamic and adaptive way in training, testing and fine-tuning. AN can be used as a drop-in replacement for existing feature normalization schema. In experiments, the proposed AN is tested in ImageNet and MS-COCO with three representative networks (ResNets, MobileNets-v2 and

AOGNets). It consistently obtains better performance, often by a large margin, than the vanilla feature normalization schema and some state-of-the-art variants.

Acknowledgement

This work was supported in part by NSF IIS-1909644, ARO Grant W911NF1810295, NSF IIS-1822477, and Salesforce Inaugural Deep Learning Research Grant (2018). The views presented in this paper are those of the authors and should not be interpreted as representing any funding agencies.

References

- [1] Lei Jimmy Ba, Ryan Kiros, and Geoffrey E. Hinton. Layer normalization. *CoRR*, abs/1607.06450, 2016. 1, 3
- [2] Andrew Brock, Jeff Donahue, and Karen Simonyan. Large scale gan training for high fidelity natural image synthesis. *arXiv preprint arXiv:1809.11096*, 2018. 2, 3, 7
- [3] Zhaowei Cai and Nuno Vasconcelos. Cascade R-CNN: delving into high quality object detection. In *2018 IEEE Conference on Computer Vision and Pattern Recognition, CVPR 2018, Salt Lake City, UT, USA, June 18-22, 2018*, pages 6154–6162, 2018. 7, 9, 10
- [4] Kai Chen, Jiaqi Wang, Jiangmiao Pang, Yuhang Cao, Yu Xiong, Xiaoxiao Li, Shuyang Sun, Wansen Feng, Ziwei Liu, Jiarui Xu, Zheng Zhang, Dazhi Cheng, Chenchen Zhu, Tianheng Cheng, Qijie Zhao, Buyu Li, Xin Lu, Rui Zhu, Yue Wu, Jifeng Dai, Jingdong Wang, Jianping Shi, Wanli Ouyang, Chen Change Loy, and Dahua Lin. MMDetection: Open mmlab detection toolbox and benchmark. *arXiv preprint arXiv:1906.07155*, 2019. 7, 9
- [5] Harm de Vries, Florian Strub, Jérémie Mary, Hugo Larochelle, Olivier Pietquin, and Aaron C. Courville. Modulating early visual processing by language. In *Advances in Neural Information Processing Systems 30: Annual Conference on Neural Information Processing Systems 2017, 4-9 December 2017, Long Beach, CA, USA*, pages 6597–6607, 2017. 2, 3
- [6] Lucas Deecke, Iain Murray, and Hakan Bilen. Mode normalization. In *7th International Conference on Learning Representations, ICLR 2019, New Orleans, LA, USA, May 6-9, 2019*, 2019. 2, 3
- [7] Vincent Dumoulin, Ishmael Belghazi, Ben Poole, Alex Lamb, Martín Arjovsky, Olivier Mastrogiorgio, and Aaron C. Courville. Adversarially learned inference. *CoRR*, abs/1606.00704, 2016. 2, 3
- [8] Ross Girshick. Fast R-CNN. In *Proceedings of the International Conference on Computer Vision (ICCV)*, 2015. 9
- [9] Kaiming He, Georgia Gkioxari, Piotr Dollár, and Ross B. Girshick. Mask R-CNN. In *IEEE International Conference on Computer Vision, ICCV 2017, Venice, Italy, October 22-29, 2017*, pages 2980–2988, 2017. 7, 9, 10
- [10] Kaiming He, Xiangyu Zhang, Shaoqing Ren, and Jian Sun. Delving deep into rectifiers: Surpassing human-level performance on imagenet classification. In *2015 IEEE Interna-*

- tional Conference on Computer Vision, ICCV 2015, Santiago, Chile, December 7-13, 2015*, pages 1026–1034, 2015. [7](#)
- [11] Kaiming He, Xiangyu Zhang, Shaoqing Ren, and Jian Sun. Deep residual learning for image recognition. In *IEEE Conference on Computer Vision and Pattern Recognition (CVPR)*, 2016. [1](#), [3](#), [4](#), [6](#), [8](#)
- [12] Tong He, Zhi Zhang, Hang Zhang, Zhongyue Zhang, Junyuan Xie, and Mu Li. Bag of tricks for image classification with convolutional neural networks. *CoRR*, abs/1812.01187, 2018. [8](#)
- [13] Andrew Howard, Mark Sandler, Grace Chu, Liang-Chieh Chen, Bo Chen, Mingxing Tan, Weijun Wang, Yukun Zhu, Ruoming Pang, Vijay Vasudevan, Quoc V. Le, and Hartwig Adam. Searching for mobilenetv3. *CoRR*, abs/1905.02244, 2019. [6](#)
- [14] Jie Hu, Li Shen, and Gang Sun. Squeeze-and-excitation networks. *CoRR*, abs/1709.01507, 2017. [2](#), [3](#), [4](#), [8](#)
- [15] Lei Huang, Xianglong Liu, Bo Lang, Adams Wei Yu, Yongliang Wang, and Bo Li. Orthogonal weight normalization: Solution to optimization over multiple dependent stiefel manifolds in deep neural networks. In *Proceedings of the Thirty-Second AAAI Conference on Artificial Intelligence (AAAI-18), the 30th innovative Applications of Artificial Intelligence (IAAI-18), and the 8th AAAI Symposium on Educational Advances in Artificial Intelligence (EAAI-18), New Orleans, Louisiana, USA, February 2-7, 2018*, pages 3271–3278, 2018. [3](#)
- [16] Lei Huang, Dawei Yang, Bo Lang, and Jia Deng. Decorrelated batch normalization. In *2018 IEEE Conference on Computer Vision and Pattern Recognition, CVPR 2018, Salt Lake City, UT, USA, June 18-22, 2018*, pages 791–800, 2018. [1](#), [3](#)
- [17] Zilong Huang, Xinggang Wang, Lichao Huang, Chang Huang, Yunchao Wei, and Wenyu Liu. Ccnet: Criss-cross attention for semantic segmentation. *CoRR*, abs/1811.11721, 2018. [2](#)
- [18] Sergey Ioffe. Batch renormalization: Towards reducing minibatch dependence in batch-normalized models. In *Advances in Neural Information Processing Systems 30: Annual Conference on Neural Information Processing Systems 2017, 4-9 December 2017, Long Beach, CA, USA*, pages 1945–1953, 2017. [1](#), [3](#)
- [19] Sergey Ioffe and Christian Szegedy. Batch normalization: Accelerating deep network training by reducing internal covariate shift. In David Blei and Francis Bach, editors, *Proceedings of the 32nd International Conference on Machine Learning (ICML-15)*, pages 448–456. JMLR Workshop and Conference Proceedings, 2015. [1](#), [3](#), [6](#), [7](#)
- [20] Songhao Jia, Ding-Jie Chen, and Hwann-Tzong Chen. Instance-level meta normalization. In *IEEE Conference on Computer Vision and Pattern Recognition, CVPR 2019, Long Beach, CA, USA, June 16-20, 2019*, pages 4865–4873, 2019. [1](#), [3](#)
- [21] M. M. Kalayeh and M. Shah. Training faster by separating modes of variation in batch-normalized models. *IEEE Transactions on Pattern Analysis and Machine Intelligence*, pages 1–1, 2019. [2](#), [3](#)
- [22] Tero Karras, Samuli Laine, and Timo Aila. A style-based generator architecture for generative adversarial networks. *arXiv preprint arXiv:1812.04948*, 2018. [2](#), [3](#)
- [23] Alex Krizhevsky, Ilya Sutskever, and Geoffrey E. Hinton. Imagenet classification with deep convolutional neural networks. In *Neural Information Processing Systems (NIPS)*, pages 1106–1114, 2012. [4](#)
- [24] Xilai Li, Xi Song, and Tianfu Wu. Aognets: Compositional grammatical architectures for deep learning. In *IEEE Conference on Computer Vision and Pattern Recognition, CVPR 2019, Long Beach, CA, USA, June 16-20, 2019*, pages 6220–6230, 2019. [1](#), [3](#), [7](#)
- [25] Tsung-Yi Lin, Piotr Dollár, Ross B. Girshick, Kaiming He, Bharath Hariharan, and Serge J. Belongie. Feature pyramid networks for object detection. In *2017 IEEE Conference on Computer Vision and Pattern Recognition, CVPR 2017, Honolulu, HI, USA, July 21-26, 2017*, pages 936–944, 2017. [9](#)
- [26] Tsung-Yi Lin, Michael Maire, Serge J. Belongie, Lubomir D. Bourdev, Ross B. Girshick, James Hays, Pietro Perona, Deva Ramanan, Piotr Dollár, and C. Lawrence Zitnick. Microsoft COCO: common objects in context. *CoRR*, abs/1405.0312, 2014. [1](#), [3](#), [6](#), [9](#)
- [27] Ilya Loshchilov and Frank Hutter. SGDR: stochastic gradient descent with restarts. *CoRR*, abs/1608.03983, 2016. [8](#)
- [28] Ping Luo, Jiamin Ren, and Zhanglin Peng. Differentiable learning-to-normalize via switchable normalization. *CoRR*, abs/1806.10779, 2018. [1](#), [2](#), [3](#), [7](#), [8](#), [9](#), [10](#)
- [29] Takeru Miyato and Masanori Koyama. cgans with projection discriminator. *arXiv preprint arXiv:1802.05637*, 2018. [2](#)
- [30] Taesung Park, Ming-Yu Liu, Ting-Chun Wang, and Jun-Yan Zhu. Semantic image synthesis with spatially-adaptive normalization. In *IEEE Conference on Computer Vision and Pattern Recognition, CVPR 2019, Long Beach, CA, USA, June 16-20, 2019*, pages 2337–2346, 2019. [2](#), [3](#)
- [31] Chao Peng, Tete Xiao, Zeming Li, Yuning Jiang, Xiangyu Zhang, Kai Jia, Gang Yu, and Jian Sun. Megdet: A large mini-batch object detector. In *2018 IEEE Conference on Computer Vision and Pattern Recognition, CVPR 2018, Salt Lake City, UT, USA, June 18-22, 2018*, pages 6181–6189, 2018. [3](#)
- [32] Ethan Perez, Harm de Vries, Florian Strub, Vincent Dumoulin, and Aaron C. Courville. Learning visual reasoning without strong priors. *CoRR*, abs/1707.03017, 2017. [2](#), [3](#)
- [33] Shaoqing Ren, Kaiming He, Ross Girshick, and Jian Sun. Faster R-CNN: Towards real-time object detection with region proposal networks. In *Neural Information Processing Systems (NIPS)*, 2015. [9](#)
- [34] Olga Russakovsky, Jia Deng, Hao Su, Jonathan Krause, Sanjeev Satheesh, Sean Ma, Zhiheng Huang, Andrej Karpathy, Aditya Khosla, Michael Bernstein, Alexander C. Berg, and Li Fei-Fei. ImageNet Large Scale Visual Recognition Challenge. *Int. J. Comput. Vision (IJCV)*, 115(3):211–252, 2015. [1](#), [3](#), [6](#)
- [35] Tim Salimans and Diederik P. Kingma. Weight normalization: A simple reparameterization to accelerate training of deep neural networks. In *Advances in Neural Information*

- Processing Systems 29: Annual Conference on Neural Information Processing Systems 2016, December 5-10, 2016, Barcelona, Spain*, page 901, 2016. [3](#)
- [36] Mark Sandler, Andrew Howard, Menglong Zhu, Andrey Zhmoginov, and Liang-Chieh Chen. Mobilenetv2: Inverted residuals and linear bottlenecks. In *Proceedings of the IEEE Conference on Computer Vision and Pattern Recognition*, pages 4510–4520, 2018. [1](#), [3](#), [7](#)
- [37] Shibani Santurkar, Dimitris Tsipras, Andrew Ilyas, and Aleksander Madry. How does batch normalization help optimization? In *Advances in Neural Information Processing Systems 31: Annual Conference on Neural Information Processing Systems 2018, NeurIPS 2018, 3-8 December 2018, Montréal, Canada.*, pages 2488–2498, 2018. [3](#), [4](#), [9](#)
- [38] Wenqi Shao, Tianjian Meng, Jingyu Li, Ruimao Zhang, Yudian Li, Xiaogang Wang, and Ping Luo. Ssn: Learning sparse switchable normalization via sparsestmax. *CoRR*, abs/1903.03793, 2019. [2](#), [3](#)
- [39] Wei Sun and Tianfu Wu. Image synthesis from reconfigurable layout and style. In *International Conference on Computer Vision, ICCV*, 2019. [2](#), [3](#)
- [40] Christian Szegedy, Vincent Vanhoucke, Sergey Ioffe, Jonathon Shlens, and Zbigniew Wojna. Rethinking the inception architecture for computer vision. *CoRR*, abs/1512.00567, 2015. [8](#)
- [41] Dmitry Ulyanov, Andrea Vedaldi, and Victor S. Lempitsky. Instance normalization: The missing ingredient for fast stylization. *CoRR*, abs/1607.08022, 2016. [1](#), [3](#)
- [42] Fei Wang, Mengqing Jiang, Chen Qian, Shuo Yang, Cheng Li, Honggang Zhang, Xiaogang Wang, and Xiaoou Tang. Residual attention network for image classification. In *2017 IEEE Conference on Computer Vision and Pattern Recognition, CVPR 2017, Honolulu, HI, USA, July 21-26, 2017*, pages 6450–6458, 2017. [3](#)
- [43] Xiaolong Wang, Ross B. Girshick, Abhinav Gupta, and Kaiming He. Non-local neural networks. In *2018 IEEE Conference on Computer Vision and Pattern Recognition, CVPR 2018, Salt Lake City, UT, USA, June 18-22, 2018*, pages 7794–7803, 2018. [2](#)
- [44] Sanghyun Woo, Jongchan Park, Joon-Young Lee, and In So Kweon. CBAM: convolutional block attention module. In *Computer Vision - ECCV 2018 - 15th European Conference, Munich, Germany, September 8-14, 2018, Proceedings, Part VII*, pages 3–19, 2018. [3](#)
- [45] Yuxin Wu and Kaiming He. Group normalization. In *Computer Vision - ECCV 2018 - 15th European Conference, Munich, Germany, September 8-14, 2018, Proceedings, Part XIII*, pages 3–19, 2018. [1](#), [3](#), [5](#), [7](#), [8](#), [9](#), [10](#)
- [46] Hongyi Zhang, Moustapha Cissé, Yann N. Dauphin, and David Lopez-Paz. mixup: Beyond empirical risk minimization. In *6th International Conference on Learning Representations, ICLR 2018, Vancouver, BC, Canada, April 30 - May 3, 2018, Conference Track Proceedings*, 2018. [8](#)
- [47] Hongyi Zhang, Yann N. Dauphin, and Tengyu Ma. Fixup initialization: Residual learning without normalization. *CoRR*, abs/1901.09321, 2019. [8](#)